

ARL-TM-80-5

**LEVEL**

**1**

Copy No. **25**

**CHARACTERISTICS OF THE ARL:UT MOVING SOURCE  
VERTICAL LINE ARRAY PROAGATION MODEL (OBERON)**

Terry L. Foreman  
Susan G. Payne

**APPLIED RESEARCH LABORATORIES  
THE UNIVERSITY OF TEXAS AT AUSTIN  
POST OFFICE BOX 8029, AUSTIN, TEXAS 78712**

ADA084824

5 March 1980

Technical Memorandum

**APPROVED FOR PUBLIC RELEASE;  
DISTRIBUTION UNLIMITED.**

*Prepared for:*

**NAVAL OCEAN RESEARCH  
AND DEVELOPMENT ACTIVITY  
NSTL STATION, MS 39529**

**DTIC  
ELECTE  
MAY 28 1980**



**DDC FILE COPY**

**80 5 23 - 042**

UNCLASSIFIED

SECURITY CLASSIFICATION OF THIS PAGE (When Data Entered)

REPORT DOCUMENTATION PAGE		READ INSTRUCTIONS BEFORE COMPLETING FORM
1. REPORT NUMBER	2. GOVT ACCESSION NO.	3. RECIPIENT'S CATALOG NUMBER
	AD-A084814	
4. TITLE (and Subtitle)		5. TYPE OF REPORT & PERIOD COVERED
CHARACTERISTICS OF THE ARL-UT MOVING SOURCE VERTICAL LINE ARRAY PROPAGATION MODEL (OBERON)		technical memorandum
7. AUTHOR(s)		6. PERFORMING ORG. REPORT NUMBER
Terry L./Foreman Susan G./Payne		ARL-TM-80-5
		8. CONTRACT OR GRANT NUMBER(s)
		N00014-78-C-0329
9. PERFORMING ORGANIZATION NAME AND ADDRESS		10. PROGRAM ELEMENT, PROJECT, TASK AREA & WORK UNIT NUMBERS
Applied Research Laboratories The University of Texas at Austin Austin, Texas 78712		(12) 377
11. CONTROLLING OFFICE NAME AND ADDRESS		12. REPORT DATE
Naval Ocean Research and Development Activity NSTL Station, Mississippi 39529		5 Mar 1980
14. MONITORING AGENCY NAME & ADDRESS (if different from Controlling Office)		13. NUMBER OF PAGES
		39
		15. SECURITY CLASS. (of this report)
		UNCLASSIFIED
		15a. DECLASSIFICATION/DOWNGRADING SCHEDULE
16. DISTRIBUTION STATEMENT (of this Report)		
Approved for public release; distribution unlimited.		
17. DISTRIBUTION STATEMENT (of the abstract entered in Block 20, if different from Report)		
(1) Technical memo.		
18. SUPPLEMENTARY NOTES		
19. KEY WORDS (Continue on reverse side if necessary and identify by block number)		
moving source                      beam spectrum vertical line array                normal mode Doppler                                computer model beam form		
ABSTRACT (Continue on reverse side if necessary and identify by block number)		
This report describes a moving source vertical line array model based on normal mode theory. A stationary vertical line array consisting of omnidirectional receiver elements is insonified by a point time harmonic source moving with constant speed and direction. The acoustic field generated by the source is computed using normal mode theory with Doppler corrections. The computer model computes beam spectra and features array steering, shading, and Doppler effects such as line shifting and broadening.		

DD FORM 1 JAN 73 1473

EDITION OF 1 NOV 65 IS OBSOLETE

UNCLASSIFIED

SECURITY CLASSIFICATION OF THIS PAGE (When Data Entered)

# TABLE OF CONTENTS

	<u>Page</u>
LIST OF FIGURES	v
1 Introduction	1
2.0 Physical Basis of the Model	3
2.1 Environment	3
2.2 Sources	5
2.3 Vertical Line Array Configuration	5
3.0 Mathematical Description	7
3.1 Calculation of Doppler Corrected Time Series	7
3.2 Definition of Array Response	9
3.3 Calculation of Beam Spectra	9
4.0 Software Description	11
4.1 Time Series Generation	11
4.2 Beamforming	15
5 Examples	17
6 Testing	29
7 Conclusions	31
ACKNOWLEDGMENTS	33
REFERENCES	35

Accession For	
NTIS GRA&I	<input checked="" type="checkbox"/>
DDC TAB	<input type="checkbox"/>
Unannounced	<input type="checkbox"/>
Justification	
By _____	
Distribution/	
Availability Codes	
Dist	Avail and/or special
A	

## LIST OF FIGURES

<u>Figure</u>	<u>Title</u>	<u>Page</u>
1	Geometry of Doppler Corrected Vertical Line Array Model	4
2	Schematic Illustration of the Organization of the Model OBERON	12
3	Flow Diagram of the Time Series Generator RANGDOP	13
4	Flow Diagram of the Beamformer BSPECR	16
5	Acoustic Environment of Vertical Line Array	18
6	Depth Variation of Acoustic Field Over Array Aperture	19
7	Plane Wave Beam Pattern of Vertical Line Array	20
8	Beam Spectra as a Function of Source Track Range from CPA	22
9	Broadside Beam Spectrum for Source Track 21.4 km from CPA	23
10	Propagation Loss for Moving and Stationary Sources	24
11	Beam Spectra as a Function of Array Steering Angle	26
12	Beam Output for Moving and Stationary Sources	27

## 1 Introduction

In 1978 the ARL:UT acoustic vertical line array model was developed under NORDA Code 520 sponsorship to aid in the analysis of PAR (programmable acoustic recorder) data. That model computes the response of a vertical line array to a stationary point cw source by performing phase shift (time delay) beamforming on the element outputs (Foreman, 1980). Acoustic fields at the elements are computed using normal mode theory rather than ray theory in order to account for the effects of bottom interaction and the curvature and inhomogeneity of wave fronts over the array aperture.

In 1979 the Doppler corrected vertical line array model OBERON was developed in order to extend vertical line array modeling capability to include the effects of source motion. The model is based on a normal mode theory of Doppler effects (Hawker, 1979) for a horizontally stratified time independent medium and a source moving with constant speed and direction along a nonradial path with respect to a fixed receiver.

The computer programs which collectively form the OBERON package calculate the pressure field produced by a moving source over an extended period of time for each element in an array. The receiver element responses are summed, according to the user's shading and steering requirements, to produce the beamformed array response. A Fourier transform is then applied to form a beam spectrum. The purpose of the OBERON program package is to compute and display beam spectra of moving sources as the source traverses one or more tracks.

The decision to base OBERON on normal mode theory and to include source motion effects, rather than resorting to more conventional ray theory and stationary source array modeling methods, was based on several considerations. Normal mode theory readily includes sediments and substrate, while ray theory models must generally rely on less accurate plane wave reflection coefficient representations of the bottom. Moreover, normal mode theory can account for the differences in Doppler broadening which can occur across the aperture of a moderate length vertical line array. Ray theory calculations tend to be inaccurate near boundaries, yet receiver arrays are often moored near the bottom. Finally, the response of an array over an extended period to a moving source will be seen to be significantly different from the response of an array to a stationary source because of range averaging effects. For all of these reasons, OBERON is suited to the prediction of array behavior under experimental conditions and can be used to simulate array responses in the absence of experimental data.

This report summarizes the mathematical description of OBERON and describes the computer programs which implement the model. Because this report is intended for general distribution, no attempt is made here to describe the use of the computer programs which make up OBERON, nor is a copy of the computer code included.

## 2.0 Physical Basis of the Model

Figure 1 shows the coordinate system, geometry, and conventions used in OBERON to specify array positions, array configurations, steering angles, and sources. The environment in which OBERON operates is also illustrated. Each of the components in this figure is described fully in the following sections.

### 2.1 Environment

The sources and vertical line arrays are immersed in an ocean overlying fluid sediment layers which in turn overlie a (possibly) solid substrate. All hydroacoustic and geoaoustic parameters of the ocean and sediments are restricted to depth variations only; no range dependence is permitted. The substrate is homogeneous.

The acoustic parameters treated in the model are density,  $\rho(z)$ , sound speed,  $c(z)$ , attenuation,  $\alpha(z)$  and, in the substrate only, shear speed,  $c_s$ , and shear attenuation,  $\alpha_s$ .

Density is constant throughout the water column and within each of the sediment layers and the substrate, although density discontinuities may exist at layer interfaces.

Sound speeds are permitted to vary arbitrarily as a function of depth in the water column and sediment layers. Sound speed discontinuities may occur at layer interfaces.

Depth variation of attenuation in the sediment layers, with discontinuities at interfaces, is also allowed, but the water itself is treated as a lossless medium. This is consistent with the low frequencies for which the model was designed and could easily be generalized.

The substrate is characterized by its density, sound speed, attenuation, shear speed, and shear attenuation.

The coordinate system is chosen so that the surface of the ocean coincides with the x-y plane and depth increases along the positive z axis. The sea surface, the water-sediment interface, the interfaces between sediment layers, and the sediment-substrate interface are all smooth, planar, and parallel. In short, the entire environment is horizontally stratified to ensure the applicability of ordinary normal mode theory.

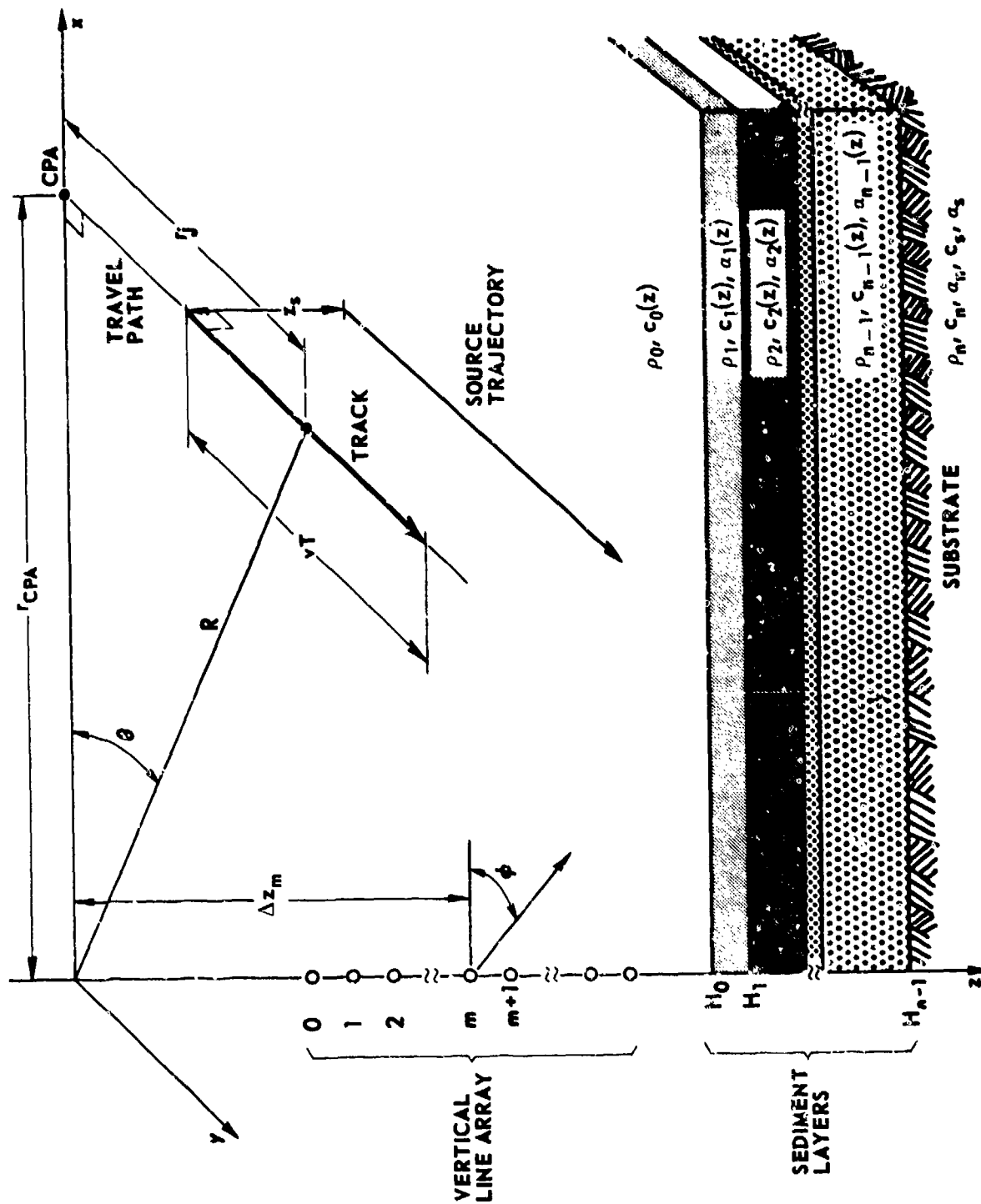


FIGURE 1  
GEOMETRY OF DOPPLER CORRECTED VERTICAL LINE ARRAY MODEL



## 2.2 Sources

OBERON computes the beam spectra resulting from point, time harmonic, omnidirectional sources moving in straight lines at constant depth  $z_s$  with constant speed  $v$ .

The projection of a source trajectory onto the surface of the ocean defines the travel path. The acoustic field generated by the source is sampled at equal time intervals  $\Delta t$  for a finite period  $T$ , during which time the source travels a distance  $vT$ . The projection of this line segment on the travel path defines the source track.

The point on the travel path nearest the origin of the coordinate system is termed the closest point of approach (CPA) of the path. Note that the source track, which is a line segment, may or may not contain CPA.

The source is specified by its angular frequency  $\omega$ , speed, depth, track length (or sample period), CPA, and range from the center of the track to CPA ( $r$ ). The track range from CPA is a signed quantity; it is negative if the source is approaching CPA and positive if the source is receding.

Time is measured with respect to the moment that the source, at a distance  $r$  from CPA and moving with speed  $v$ , would pass through CPA. Thus, time is also a signed quantity, being negative for a source approaching CPA and positive for a receding source.

## 2.3 Vertical Line Array Configuration

The vertical line array consists of one or more point, omnidirectional receiver elements distributed along the positive  $z$  axis. The array is specified by the depths of the receiver elements. Spacing between the elements is arbitrary and elements may be located within the sediment.

### 3.0 Mathematical Description

The final product of the beamforming programs of OBERON is a power spectrum for each source track and steering angle. The computations leading to these results can be divided into several stages: (1) computation of the time dependent acoustic field at each array element; (2) calculation of the array response (beamforming) at each time sample; and (3) production of the power spectrum by application of a complex fast Fourier transform to the array response.

#### 3.1 Calculation of Doppler Corrected Time Series

The derivation of the expression for the Doppler corrected time series is described in detail by Hawker (1979). The results are summarized here.

The time dependent acoustic field in a lossless medium is given by

$$\Psi(z,t) = i\rho_0(2\pi)^{1/2} e^{-i(\omega t + \pi/4)} \sum S_n(r,t) \quad (1)$$

$$S_n(r,t) = \frac{u_n(z_s) u_n(z)}{(k_n R)^{1/2}} e^{ik_n R f(\theta)} \quad (2)$$

$$f(\theta) = 1 - \frac{v}{v_n} \sin \theta + \frac{1}{2} \left( \frac{v}{v_n} \right)^2 [1 + (1-D_n) \sin^2 \theta] + \dots \quad (3)$$

$$D_n = k_n \partial v_n^G / \partial \omega, \quad (4)$$

where  $v_n^G$  is the group velocity of normal mode  $n$ ,  $u_n(z)$  is the eigenfunction corresponding to the eigenvalue  $k_n$ ,  $R$  is the range from the source position on the track to the coordinate system origin at time  $t$ , and  $\theta$  is the track bearing angle (see Fig. 1). The principal assumptions made in the derivation are that (1) the environment is horizontally stratified, (2) the source is moving in a straight line at constant speed, (3)  $k_n R \gg 1$ , and (4)  $v/v_n^G \ll 1$ .

The range invariance constraint is imposed because the Doppler corrected time series computation is based on ordinary normal mode theory.

Assuming that  $\alpha(z) \ll \omega/c(z)$ , the loss due to absorption is accounted for to first order by adding a small perturbation term  $i\delta_n$  to the eigenvalue, where

$$\delta_n = \beta_n + \beta_s + \sum_1^L \beta_i \quad (5)$$

$$\beta_i = \rho_i \frac{\omega}{k_n} \int_{H_{i-1}}^{H_i} \frac{\alpha_i(z)}{c_i(z)} u_n^2(z) dz \quad (6)$$

$$\beta_n = \alpha_n \gamma_n \quad (7)$$

$$\beta_s = \alpha_s \gamma_s \quad (8)$$

where  $H_i$  is the depth of layer  $i$  (see Fig. 1),  $\gamma_s$  and  $\gamma_n$  are first order shear and compressional perturbation factors, and  $n$  is the number of sediment layers. Retaining only first order perturbation terms, Eq. (1) can be written to include absorption:

$$\psi(z,t) = i\rho_0 (2\pi)^{1/2} e^{-i(\omega t + \pi/4)} \sum S_n(r,t) e^{-\delta_n R} \quad (9)$$

Repeated evaluation of Eq. (9) at array element depth  $z$  at fixed time intervals as the source moves along the track yields the complex time series for that element.

The normal mode quantities  $u_n(z)$  and  $k_n$  (Eqs. (2), (6), and (9)) are obtained from the solutions to the depth separated wave equation

$$\frac{d^2 u_n(z)}{dz^2} + (k^2(z) - k_n^2) u_n(z) = 0 \quad (10)$$

A description of the normal mode solution, and the calculation of  $v_n^G$ ,  $\gamma_n$ , and  $\gamma_n$  is given by Gonzalez (1980).

### 3.2 Definition of Array Response

The response of the vertical line array at time  $t$  is the sum of each of the array element responses at time  $t$  weighted by their respective shading and steering coefficients:

$$R(\phi, t) = \sum_m s_m w_m(\phi) \psi(z_m, t) \quad , \quad (11)$$

where  $\phi$  is the steering elevation/depression angle,  $s_m$  are real amplitude shading coefficients, and the  $w_m$  are complex steering coefficients.

The amplitude shading coefficients  $s_m$  are assumed to be equal unless the user supplies other values in an attempt to reduce sidelobes. In any event, the coefficients are rescaled if necessary so that their sum is unity.

The plane wave steering coefficients  $w_m$  are given by Urlick (1967),

$$w_m = e^{-ik(z_m - z_0)\sin \phi} \quad , \quad (12)$$

$$\text{where} \quad k = 2\pi f/c \quad . \quad (13)$$

### 3.3 Calculation of Beam Spectra

If the array response is calculated as shown in the preceding section for each of  $N$  time samples at constant time intervals  $\Delta t$ , the result is an array response time series. The array response time series thus formed may then be transformed using a standard complex fast Fourier transform (FFT) routine (Brigham, 1974). The bandwidth of the resulting spectrum is  $1/\Delta t$  and the frequency resolution is  $1/N\Delta t$ .

The sidelobes appearing in the array response spectrum may be suppressed in OBERON by the optional application of a Hanning complex digital filter (Brigham, 1974) at the cost of reduced frequency resolution.

#### 4.0 Software Description

OBERON is a collection of computer programs that perform the three step process, described in Sec. 3.0, under control of the ARL:UT model operating system (Payne, 1980). These programs communicate through disk files. There are five main programs in the OBERON package: NEMESIS, RANGDOP, DOPFMT, BSPEC, and DOPPLT. The roles of these programs are discussed in the following sections. The organization of the program package is illustrated in Fig. 2.

The modular structure of OBERON promotes flexibility of application for the user and simplifies modification of the model. For example the time series generator, RANGDOP, could be replaced with another program which computes the field differently, or a measured or computed ambient noise field could be added to the cw source generated field without altering the OBERON package.

#### 4.1 Time Series Generation

Before a time series can be generated the ARL:UT normal mode model NEMESIS is run with a user supplied hydroacoustic and geoacoustic description of the environment and the source frequency. It produces a computer disk file containing  $k_n$ ,  $u_n(z)$ ,  $v_n^G$ ,  $\gamma_s$ , and  $\gamma_n$  for each normal mode  $n$ . Gonzalez (1980) describes this model.

RANGDOP is then run to compute the complex time dependent acoustic field  $\Psi(z,t)$ . Figure 3 is a flow diagram of the procedure. The program reads the disk file produced by NEMESIS and the user supplied values of attenuation, source speed, source depth, range to CPA, array element depths, number of points to calculate in the time series ( $M$ ), the range of the center of the track from CPA ( $r$ ), and the sample rate. Using Eq. (9) the field is computed from time  $t_c - M\Delta t/2$  to  $t_c + M\Delta t/2$  at  $\Delta t$  intervals for each source, array element, and track, where  $t_c = r/v$ . The results are written on a disk file.

Computing the time series can be expensive because of the large number of calculations involved. Three measures were taken to reduce the number of calculations. The first of these was the substitution of a very rapid table lookup and linear interpolation procedure for the standard FORTRAN sine and cosine routines.

The second was the inclusion in RANGDOP of a discrimination process for identifying terms in Eq. (1) which would make insignificant contributions to the field and deleting such terms from the summation of Eq. (1). A term  $S_n(r,t)$  can be neglected if and only

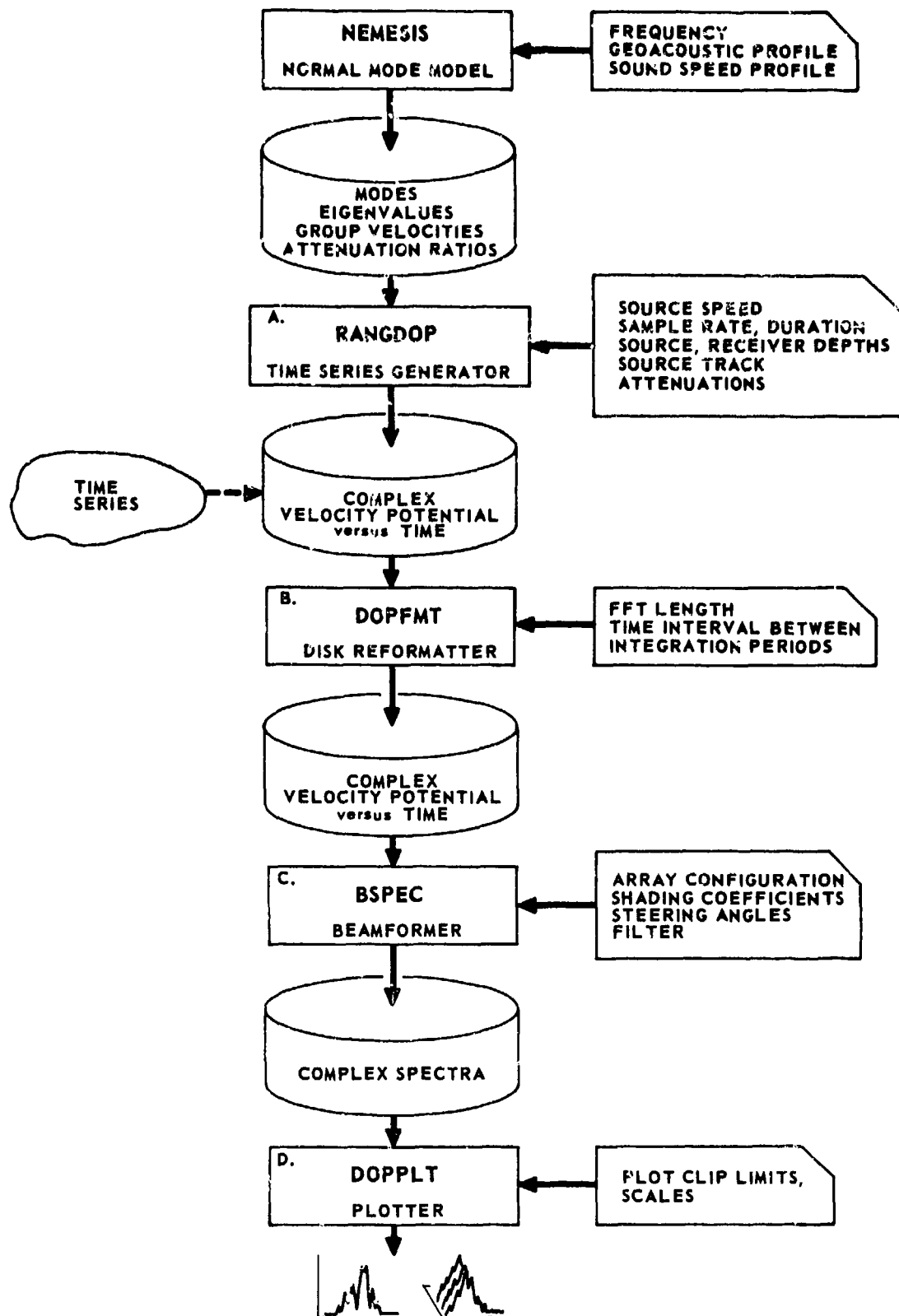


FIGURE 2  
SCHEMATIC ILLUSTRATION OF THE ORGANIZATION OF THE MODEL OBERON

ARL:UT  
AS-80-681  
TLF-GA  
2-5-80

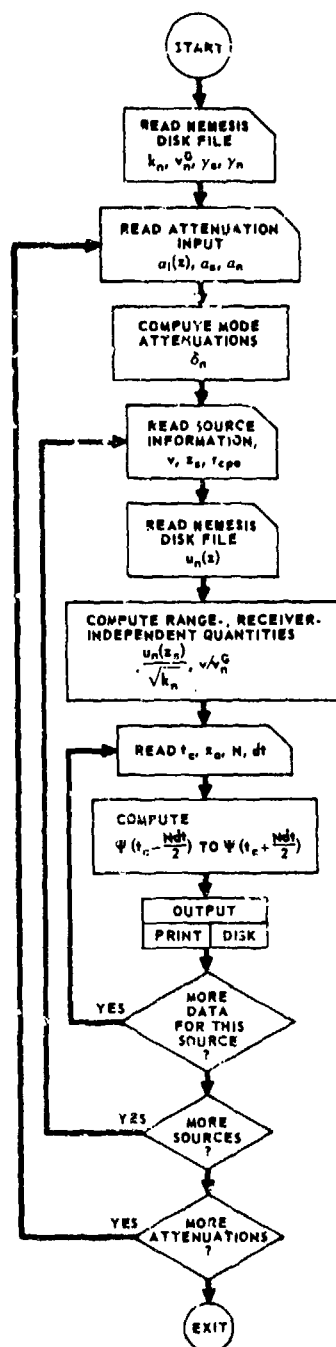


FIGURE 3  
FLOW DIAGRAM OF THE TIME SERIES GENERATOR RANGDOP



If its magnitude does not exceed a small positive fraction  $\epsilon$  of the magnitude of the term having the greatest magnitude for a given range  $R$ ; that is

$$|S_n(r,t)| \leq |S_m(r,t)| \epsilon \quad (14)$$

where

$$|S_m(r,t)| = \max |S_n(r,t)| \quad (15)$$

Substituting the expression for  $S_n(r,t)$  (Eq. 2), the test for term omission is written

$$A_n e^{-R\delta_n} \leq A_m e^{-R\delta_m} \quad (16)$$

where

$$A_n = \frac{|u_n(z_s) u_n(z)|}{k_n^{1/2}} \quad (17)$$

This form of the test requires that an exponential be calculated at each range. By taking logarithms the test is cast in a form which requires only arithmetic calculations at each range:

$$a_n - R\delta_n \leq \tau(R) + \ln \epsilon \quad (18)$$

$$\tau(R) = a_m - R\delta_m \quad , \text{ and} \quad (19)$$

$$a_n = \ln A_n \quad (20)$$

The last efficiency improvement was the development of a time series reformatting program DOPFMT. This program reformats the time series produced by RANGDOP into a form accessible to the beamformers. With this program a time series several hours long can be split into separate source tracks of user-specified duration, each with a user-specified time delay between the start of successive tracks. DOPFMT can, if requested, produce disk files of time series generated by overlapping source tracks, yet no redundant time series calculations are performed. Time series from overlapping source tracks are often supplied as input to the beamformers. DOPFMT can also be used to extract a time series for a track of user-specified length and position from the original, possibly very long series generated by RANGDOP.

## 4.2 Beamforming

There are two beamforming programs in OBERON, BSPECR and BSPECA. Both perform identical computations and differ only in the form of output produced. The programs produce one spectrum for each array steering angle and source track, and create output disk files suitable for display or further processing.

The programs require user input specifying the shading coefficients, steering angles, filter requirements, and array element depths. The required time series are read from the disk file produced by DOPFIT.

BSPECR produces spectra for one array steering angle and a series of source ranges from CPA, that is, beam spectra at specified ranges. A flow diagram of the procedure appears in Fig. 4. The output can be displayed using DOPPLT as a three dimensional plot showing intensity level (dB) versus frequency and source range. Alternatively, the total power in the spectrum can be computed at each range to form a moving source "propagation loss" curve (see examples).

BSPECA computes the spectra at a single source range and a series of steering angles. The results can be exhibited as a three dimensional plot showing intensity versus frequency and steering angle. Plotting the total power in the spectrum as a function of grazing angle yields a moving source beam output curve.

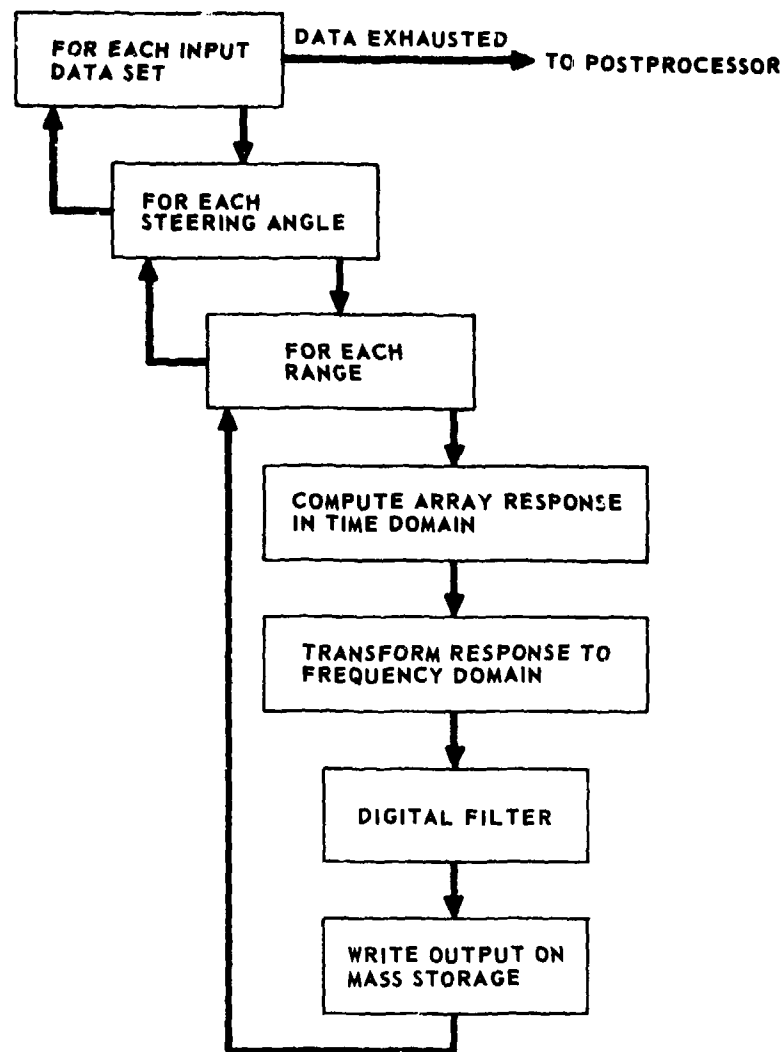


FIGURE 4  
FLOW DIAGRAM OF THE BEAMFORMER BSPECR

## 5 Examples

Typical applications of the OBERON programs are illustrated in the following examples. When appropriate, results from OBERON are compared and contrasted with results from ray theory and with results from the stationary source vertical line array model.

The sound speed profile of Fig. 5 is a typical deep ocean profile. The depth of the water column is 4883 m. The underlying 200 m sediment is a silty clay having a surficial sound speed of 1523.9 m/sec, a sound speed gradient of 1/sec, a density of 1.42 g/cc and an attenuation of 0.1 dB/m/kHz. The substrate has a sound speed of 5000 m/sec, a density of 2.6 g/cc, and an attenuation of 0.03 dB/m/kHz. All of the examples presented in this section were obtained with this acoustic environment.

Normal modes and eigenvalues were computed for the acoustic environment of Fig. 5 and a source frequency of 25 Hz using NEMESIS. All stationary and moving source wave theory calculations described below are based on these results.

Figure 6 shows acoustic field intensity versus depth in a region near the ocean bottom where a vertical line array is deployed. The field was computed assuming a stationary source 100 m below the surface at a range of 23.621 km (the choice of range will be explained later). The field is seen to vary rapidly over the array aperture.

The vertical line array consists of seven uniformly spaced receiver elements. The element spacing of 15 m corresponds to one-quarter wavelength at 25 Hz and a nominal sound speed of 1500 m/sec. The array is positioned with the deepest receiver element at a depth of 4710 m, or 173 m from the bottom.

The 25 Hz plane wave beam pattern for the array, steered broadside, is displayed in Fig. 7. The main lobe has a 3 dB beamwidth of 30 deg and the peak intensities of the sidelobes are 13 dB below the peak intensity of the main lobe. The beamwidth is narrow enough and the sidelobe suppression sufficient for the array to distinguish between groups of eigenrays with different path histories as the array is steered vertically between -45 deg and 45 deg.

At this point the array position and configuration has been established, the acoustic environment specified, and the normal modes and eigenvalues for that environment computed assuming a 25 Hz source. There remains the specification of the source to satisfy the input requirements of the time series generator, RANGDOP.

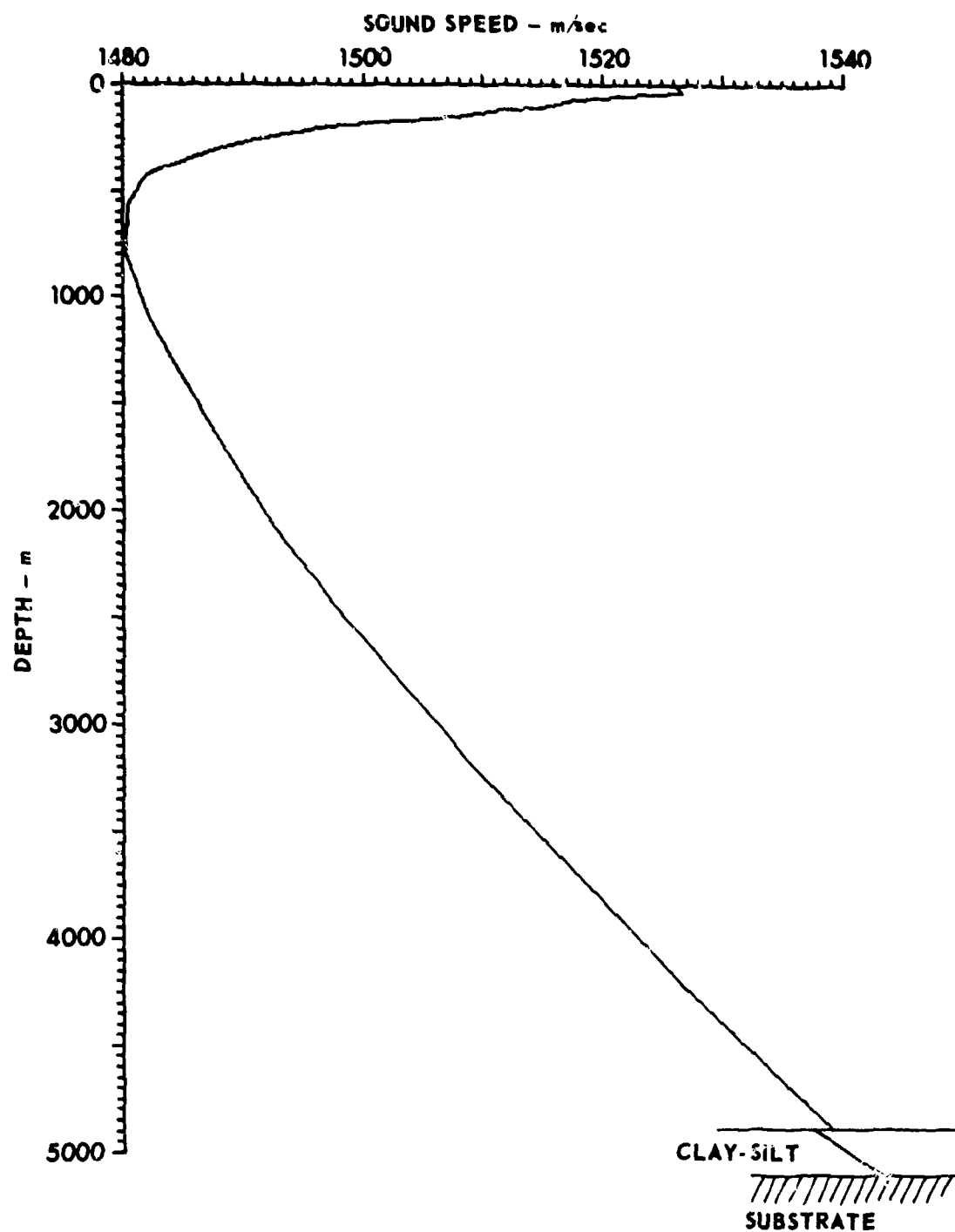


FIGURE 5  
ACOUSTIC ENVIRONMENT OF VERTICAL LINE ARRAY

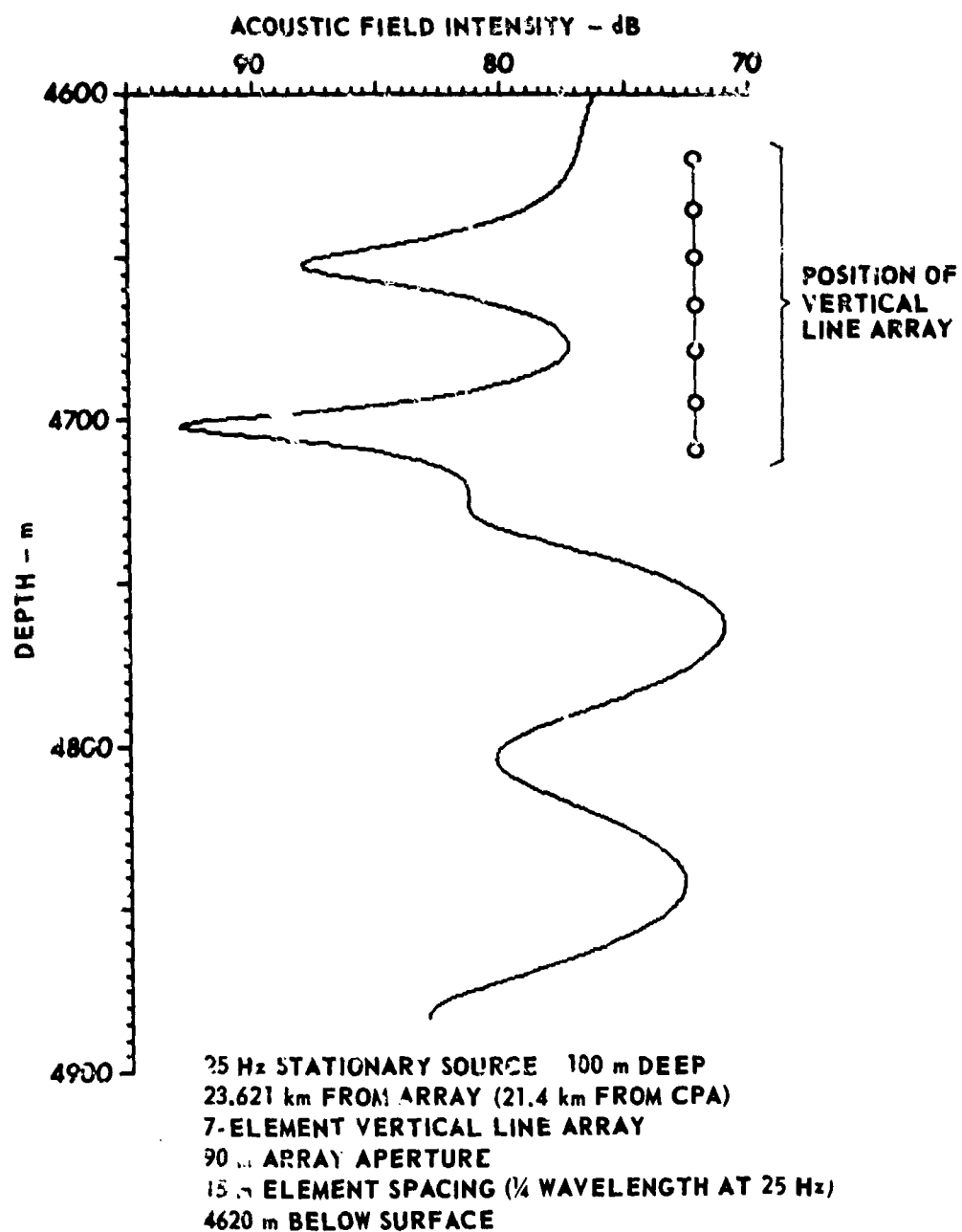


FIGURE 6  
 DEPTH VARIATION OF ACOUSTIC FIELD OVER ARRAY APERTURE

25 Hz  
7-ELEMENT VERTICAL LINE ARRAY  
90 m ARRAY APERTURE  
15 m ELEMENT SPACING  
( $\frac{1}{4}$  WAVELENGTH AT 25 Hz)

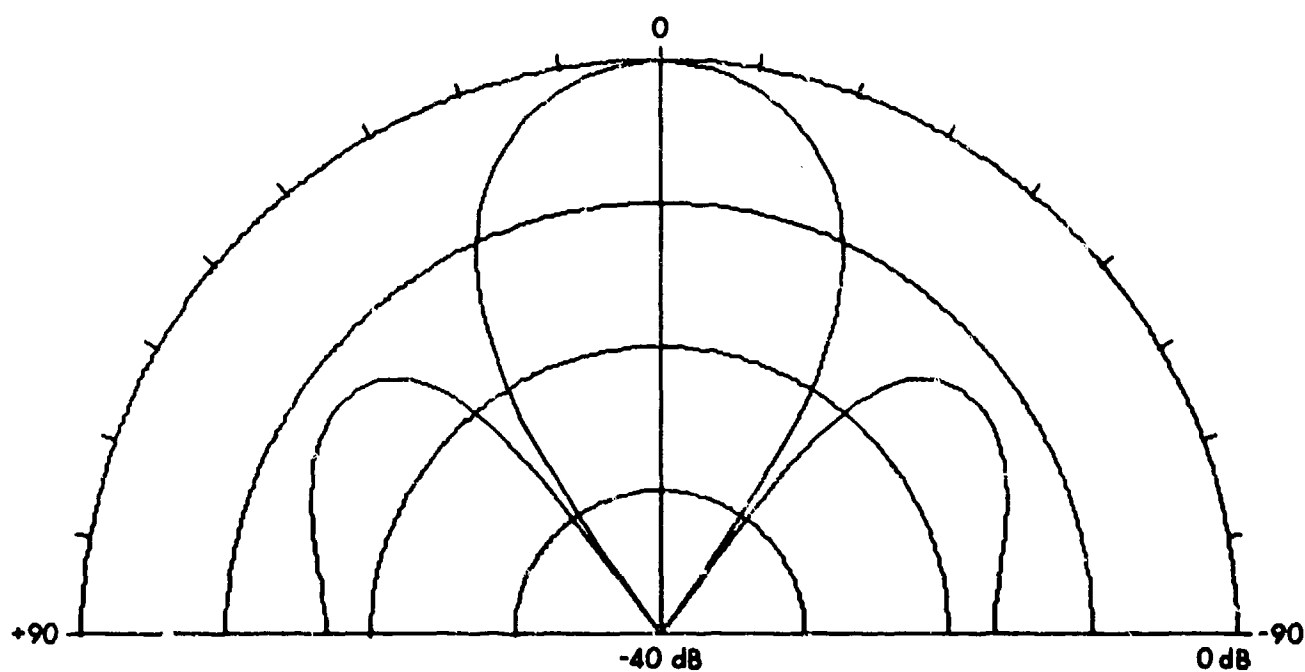


FIGURE 7  
PLANE WAVE BEAM PATTERN OF VERTICAL LINE ARRAY

The source selected travels at 10 m/sec at a depth of 100 m. Its closest point of approach to the array is 10 km. Source tracks are 12.775 km in length. The complex field generated as the source traverses a track is sampled 512 times at 2.5 sec intervals. Track centers are spaced 2.5 km apart, starting 6.4 km from CPA and ranging up to 106.4 km. The tracks overlap.

The next step in the production of beam spectra is the generation of time series for each track and receiver element, using RANGDOP and DOPFMT.

Figure 8 shows output from the beamformer BSPECR. Each line of the plot represents the array response spectrum for a different source track. The baseline of each spectrum represents a 120 dB floor (re 0 dB at 1 m) below which the response is ignored. Baselines are positioned on the plot so that the range from CPA of the track giving rise to a given spectrum can be read directly. Signal strength is indicated by height above a baseline; the scale is given by the axis to the right of the plot. It should be noted that the pressures computed by RANGDOP are scaled in the beamformers by  $1/N$  in order that the beam output levels not depend on  $N$  (the number of samples) and so that the levels will be consistent with stationary source propagation loss predictions.

One can follow the progress of the source by observing the migration and evolution of the line structure as the source recedes from the array. Doppler shifted signal frequencies decrease monotonically, approaching asymptotically the limit of the radial travel path. Signal strength decays, primarily due to geometrical spreading (bottom reflection losses are small, typically ranging from 1 to 4 dB per bottom bounce). Direct and bottom refracted paths show the greatest signal strength and undergo the largest Doppler shift; paths which reflect from the substrate show smaller Doppler shifts and are attenuated while passing through the sediment. As the source recedes, the frequency separation between direct and reflected paths increases.

The beam spectrum for the track 21.4 km from CPA and 23.621 km from the array is plotted in Fig. 9. Ray theory predictions of Doppler shifts for direct, refracted, and reflected paths are indicated. The agreement is close except when bottom image interference effects are important.

A moving source "propagation loss" curve can be obtained from the series of spectra shown in Fig. 8 by computing the total energy in each spectrum and plotting the result as propagation loss versus track range from the array. Such a curve is compared in Fig. 10 with a conventional propagation loss curve for a stationary source at the same series of ranges. Because the moving source changes position while the time series is collected the moving source propagation loss curve is range averaged and, hence, smoother than the stationary



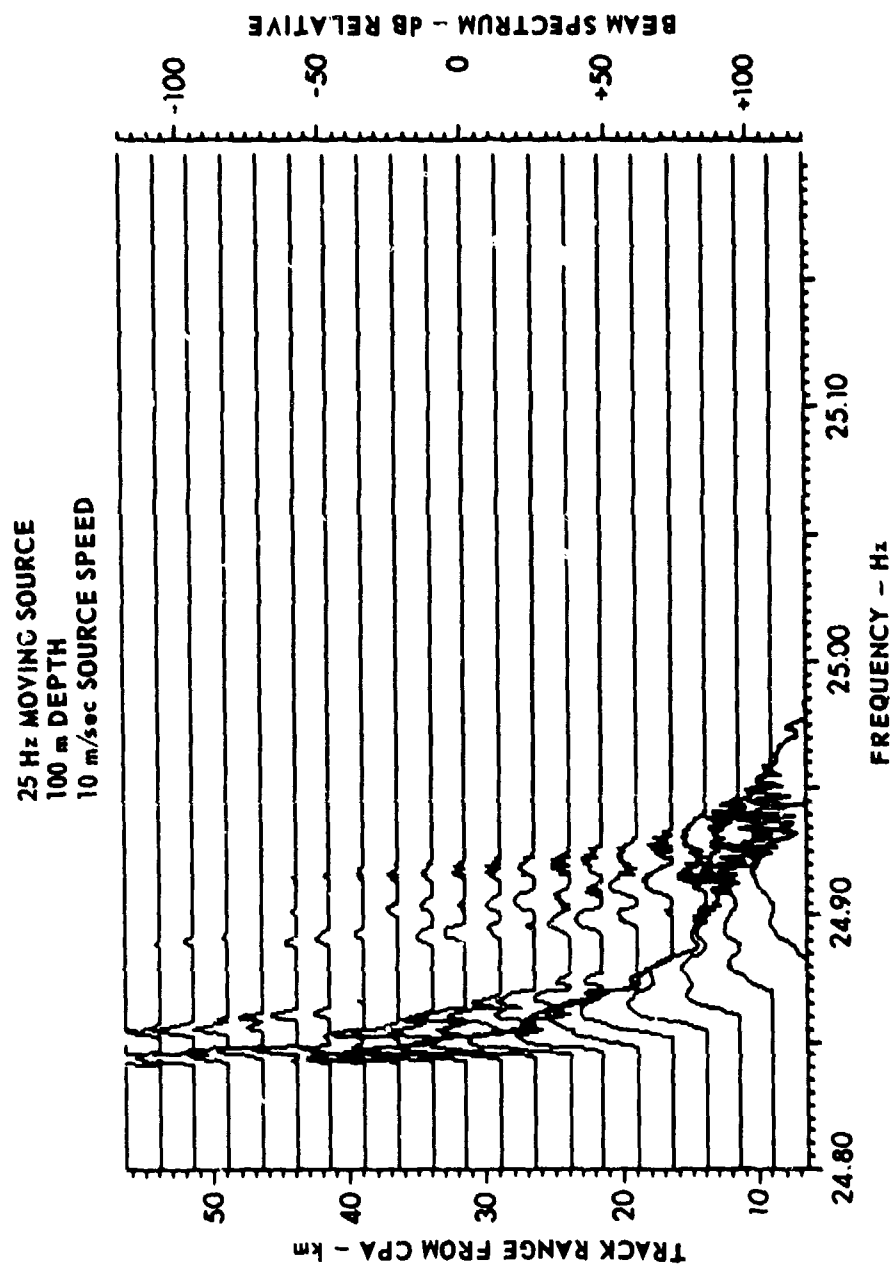


FIGURE 8  
BEAM SPECTRA AS A FUNCTION OF SOURCE TRACK RANGE FROM CPA

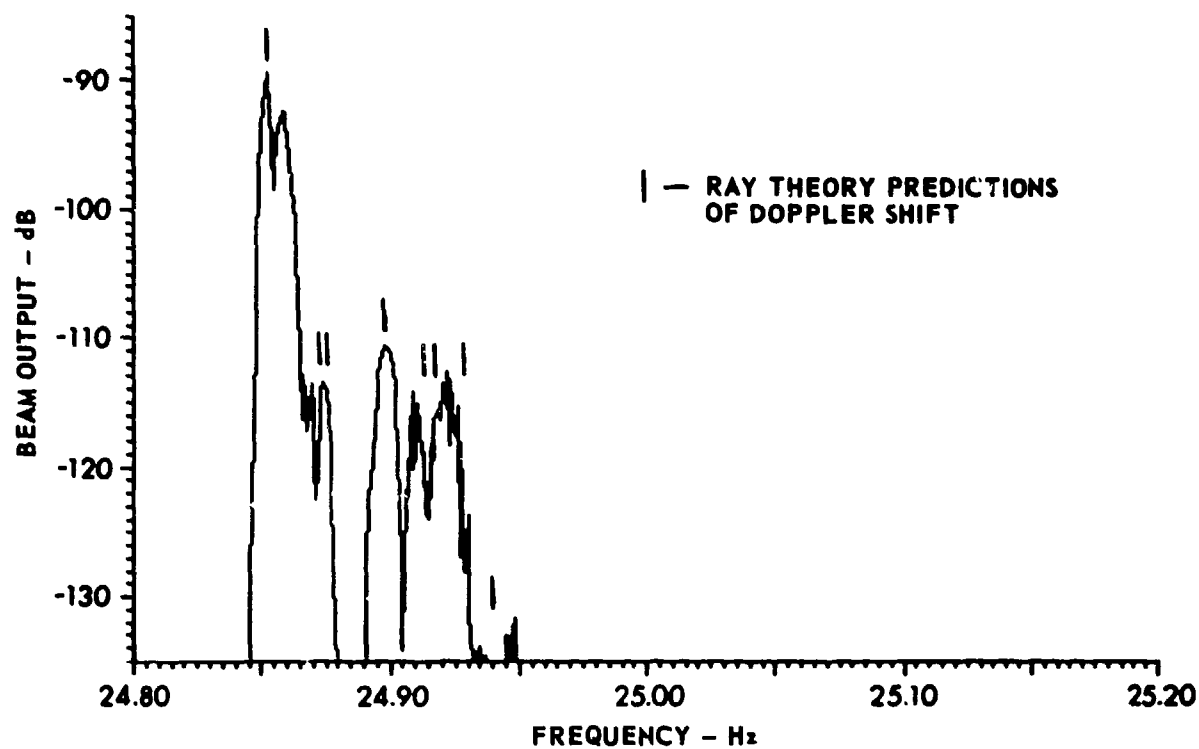


FIGURE 9  
BROADSIDE BEAM SPECTRUM FOR SOURCE TRACK 21.4 km FROM CPA

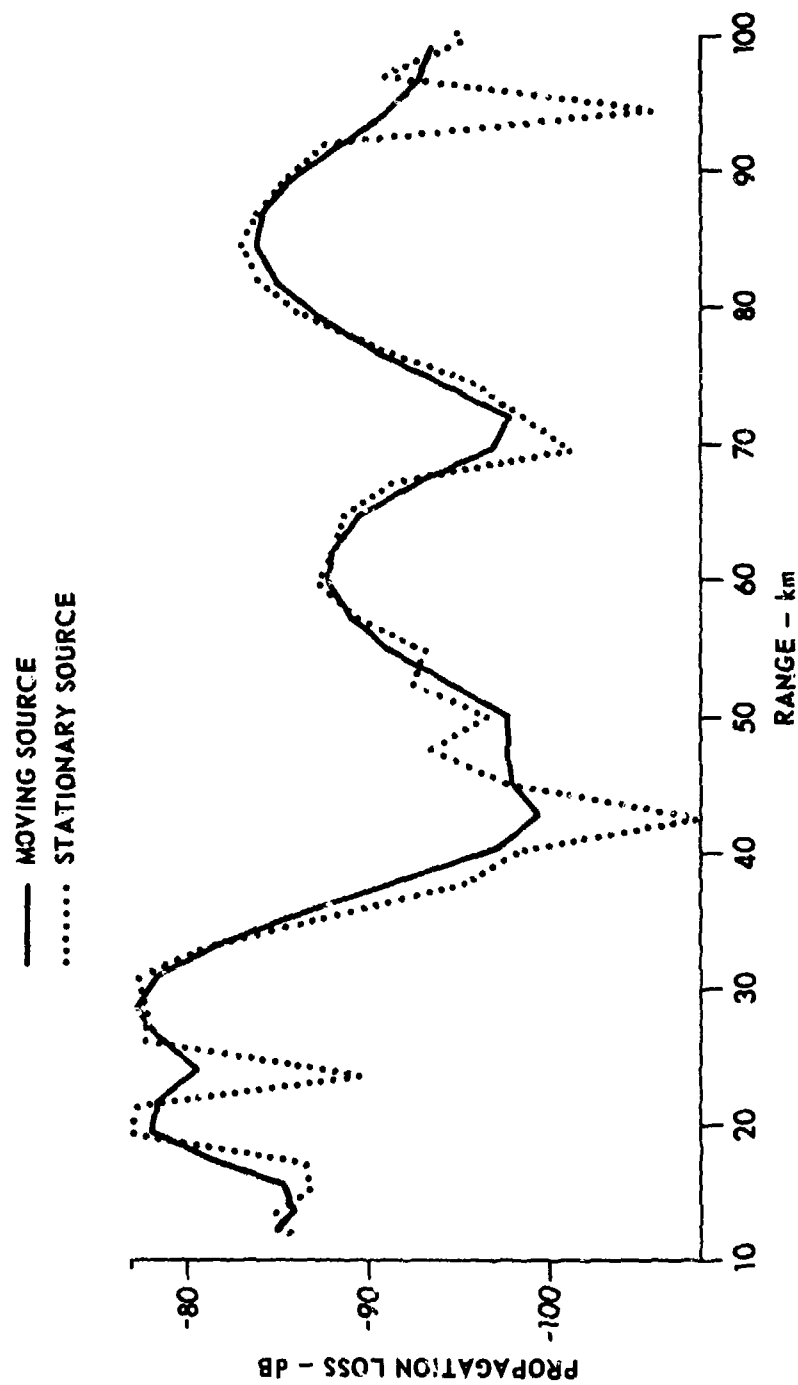


FIGURE 10  
PROPAGATION LOSS FOR MOVING AND STATIONARY SOURCES

ARL:UT  
AS-80-786  
TLF-GA  
2-12-80

source curve.

Figure 11 shows beam spectra as a function of array steering angle for a track 21.4 km from CPA and 23.621 km from the array. When the total energy of these spectra is plotted as moving source "beam output" versus array steering angle another manifestation of range averaging appears. Figure 12 shows beam output for the moving source and for three stationary sources positioned at the center and both ends of the track. Each stationary source beam output curve contains a null. The nulls occur at different array steering angles for each different source position. No such structure is discernible in the moving source beam output curve because the arrival structure varies during the source transition of the track.

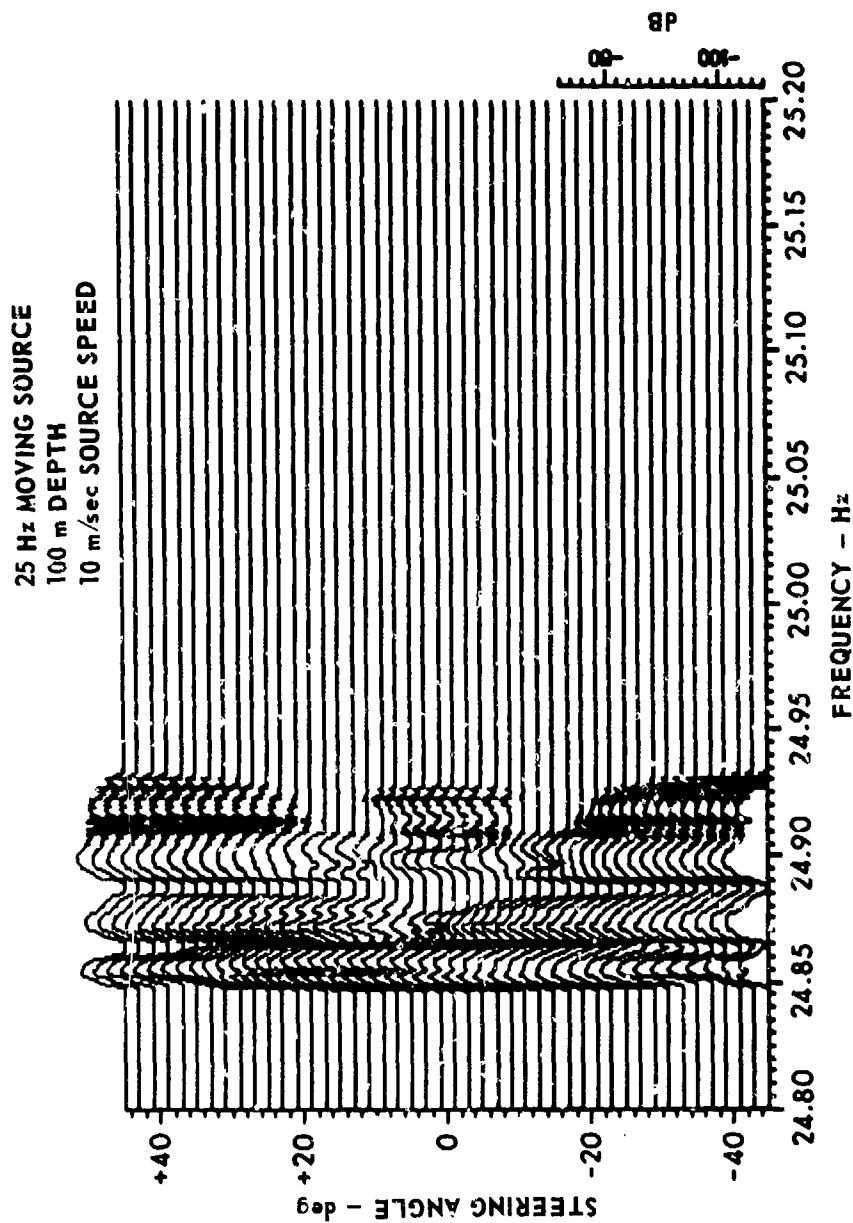


FIGURE 11  
BEAM SPECTRA AS A FUNCTION OF ARRAY STEERING ANGLE

ARL:UT  
AS-80-772  
TLF-GA  
2-7-80  
REV 5-13-80

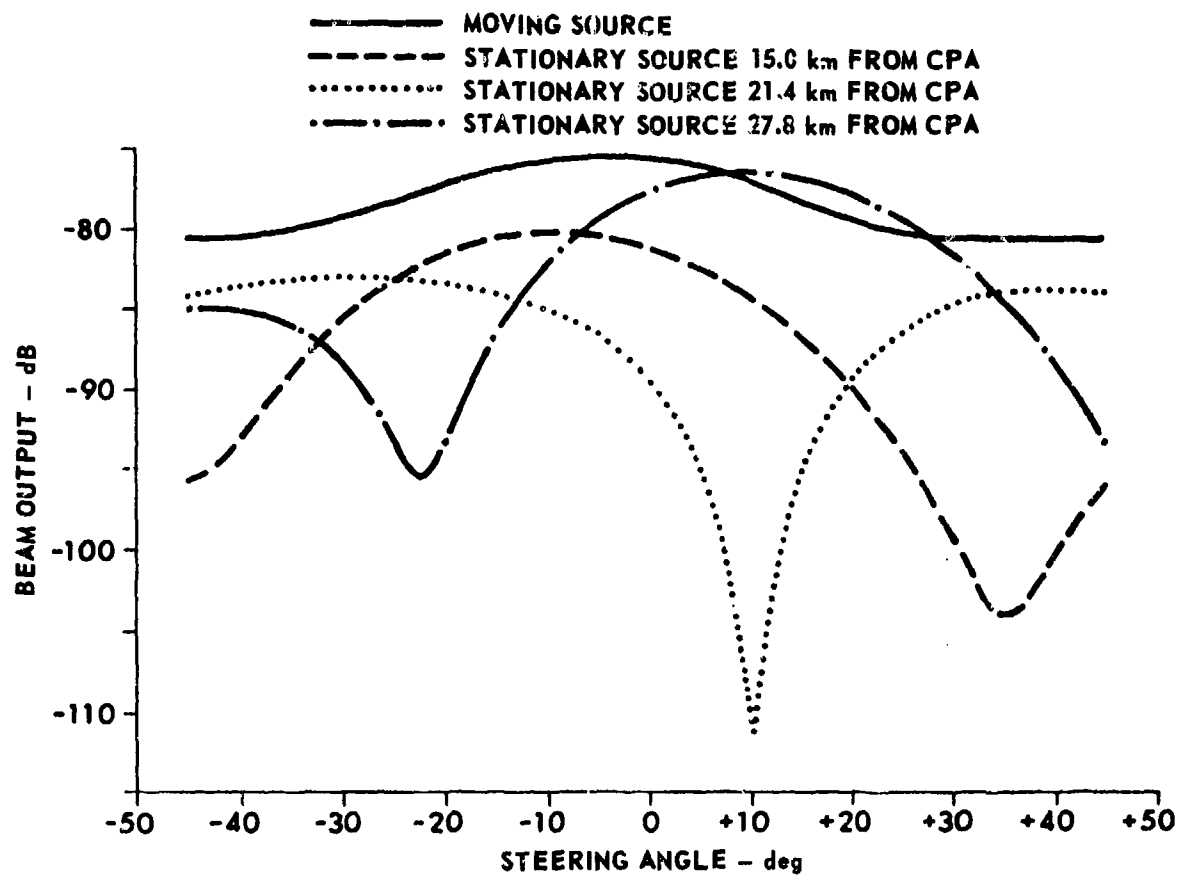


FIGURE 12  
BEAM OUTPUT FOR MOVING AND STATIONARY SOURCES

ARL:UT  
AS-80-788  
TLF-GA  
2-12-80  
REV 5-13-80

## 6 Testing

The normal mode model, NEMESIS, was exhaustively examined and tested during its development (Gonzalez, 1980).

The time series generator, RANGDOP, has been checked in several ways. The correctness of the attenuation calculations is indicated by comparisons with an independently developed bottom loss model, as discussed by Tindle (1979). The time series calculations were tested by computing the field for a very slow moving source (1 mm/sec), as well as by checks of internal consistency and parametric dependence of the output. Comparisons of the field at selected ranges with the field produced by a stationary source at the same ranges showed agreement. Analytic calculations of the Doppler shift at long ranges agreed with predictions produced by OBERON. Ray theory predictions of Doppler broadening also agreed with those of OBERON, within the limitations of ray theory.

Using the 1 mm/sec source calculations, the output from the beamforming programs was compared with the output from the stationary source vertical line array model VLAM (Foreman, 1980). Computations of power at selected ranges showed agreement with a normal mode propagation loss model.

## 7 Conclusions

A moving source vertical line array propagation model (OBERON) based on a normal mode computation of the acoustic field has been designed, programmed, tested, and made available for use. The model provides the capability for computing vertical line array responses which include the effects of source motion and layer boundaries. Possibilities for future extensions include adding measured (synoptic or archival) or modeled ambient noise to obtain a hybrid "model" of array response.



### Acknowledgments

The OBERON model was developed under the guidance of Kenneth Hawker. The normal mode program NEMESIS was designed and implemented by Ruth Gonzalez. The authors also benefited from consultation with Jack Shooter and Clark Penrod.

### References

Brigham, Oran E., The Fast Fourier Transform, (Prentice-Hall, Englewood Cliffs, N. J. 1974).

Foreman, Terry L., "Acoustic Ray Models Based on Eigenrays", Applied Research Laboratories Technical Report No. 77-1 (ARL-TR-77-1), Applied Research Laboratories, The University of Texas at Austin, 4 April 1977.

Foreman, Terry L., "Characteristics of the ARL:UT Vertical Line Array Propagation Model (VLAM)", Applied Research Laboratories Technical Report No. 80-7 (ARL-TR-80-7), Applied Research Laboratories, The University of Texas at Austin, 1980.

Gonzalez, R., "The Acoustic Normal Mode Model NEMESIS", Applied Research Laboratories Technical Memorandum No. 80-13 (ARL-TR-80-13), Applied Research Laboratories, The University of Texas at Austin, 1980.

Hawker, K. E., "Aspects of the Acoustic Bottom Interaction Problem", Applied Research Laboratories Technical Report No. 78-49 (ARL-TR-78-49), Applied Research Laboratories, The University of Texas at Austin, December 1978.

Hawker, K. E., "A Normal Mode Theory of Acoustic Doppler Effects in the Oceanic Waveguide", J. Acoust. Soc. Am. 65, 675-681 (1979).

Payne, Susan G., "A User-Oriented Model Operating System", Applied Research Laboratories Technical Memorandum No. 80-4 (ARL-TM-80-4), Applied Research Laboratories, The University of Texas at Austin, March 1980.

Tindle, C. T., "The Equivalence of Bottom Loss and Mode Attenuation per Cycle in Underwater Acoustics", J. Acoust. Soc. Am. 66, 250-256 (1979).

Urick, R. J., Principles of Underwater Sound (McGraw-Hill, New York, 1967).

5 March 1980

DISTRIBUTION LIST FOR  
ARL-TM-80-5  
UNDER CONTRACT N00014-78-C-0329

COPY NO.

Commanding Officer  
Naval Ocean Research and  
Development Activity  
Department of the Navy  
NSTL Station, MS 39529  
1 Attn: LCDR K. E. Evans, Code 520  
2 CDR J. Paquin, Code 500  
3 S. W. Marshall, Code 340  
4 A. L. Anderson, Code 320  
5 Code 520  
6 Library, Code 125

Commanding Officer  
Office of Naval Research  
Arlington, VA 22217  
7 Attn: A. Sykes, Code 222  
8 M. McKisic, Code 486

9 Office of Naval Research  
Branch Office, Chicago  
Department of the Navy  
536 South Clark Street  
Chicago, IL 60605

Commanding Officer  
Naval Electronic Systems Command  
Washington, DC 20360  
10 Attn: CDR L. Henderson, Code PME 124-30  
11 E. Chaika, Code PME 124-TA  
12 J. Sinsky, Code 320

Director  
Naval Research Laboratory  
Department of the Navy  
Washington, DC 20375  
13 Attn: B. B. Adams, Code 8160

Commanding Officer  
Naval Ocean Systems Center  
Department of the Navy  
San Diego, CA 92152  
14 Attn: E. Tunstall

Chief of Naval Operations  
Department of the Navy  
Washington, DC 20350  
15 Attn: CDR J. Hackett, OP952D

Distribution List for ARL-TM-80-5, under Contract N00014-78-C-0329 (Cont'd)

COPY NO.

16	Chief of Naval Material Department of the Navy Washington, DC 20360 Attn: CAPT. E. Young, Code 08T24
17	Naval Oceanographic Office NSTL Station, MS 39529 Attn: W. Jobst, Code 3440
18	Commander Naval Air Development Center Department of the Navy Warminster, PA 18974 Attn: P. Van Schuyler, Code 2052
19	C. Hammond
20	Defense Advanced Research Projects Agency Acoustic Research Center Moffett Field, CA 94035 Attn: E. Smith
21	Defense Advanced Research Projects Agency 1400 Wilson Boulevard Arlington, VA 22209 Attn: T. Kooij
22	Superintendent Naval Postgraduate School Monterey, CA 93940 Attn: H. Medwin
23	Library
24	Commanding Officer Naval Air Systems Command Department of the Navy Washington, DC 20361 Attn: CDK J. Messegee, Code PMA-264
25	Commanding Officer and Director Defense Technical Information Center Cameron Station, Building 5 5010 Duke Street Alexandria, VA 22314
26	Woods Hole Oceanographic Institution 86-95 Water Street Woods Hole, MA 02543 Attn: E. E. Hayes

Distribution List for ARL-TM-80-5, under Contract N00014-78-C-0329 (Cont'd)

COPY NO.

27	Science Applications, Inc.
28	8400 Westpark Drive
	McLean, VA 22101
	Attn: J. Hanna
	C. Spofford
29	Marine Physical Laboratory of
	The Scripps Institution of Oceanography
	The University of California, San Diego
	San Diego, CA 92132
	Attn: F. Fisher
30	Tracor, Inc.
	1601 Research Boulevard
	Rockville, MD 20850
	Attn: J. Gottwald
31	Planning Systems, Inc.
	7900 Westpark Drive, Suite 507
	McLean, VA 22101
	Attn: L. Solomon
32	TRW, Inc.
	TRW Defense & Space Systems Group
	Washington Operations
	7600 Colshire Drive
	McLean, Va 22101
	Attn: A. Fadness
33	Office of Naval Research
	Resident Representative
	Room No. 582, Federal Bldg.
	Austin, Texas 78701
34	Glen E. Ellis, ARL:UT
35	Terry L. Foreman, ARL:UT
36	Loyd Hampton, ARL:UT
37	Kenneth E. Hawker, ARL:UT
38	Steven K. Mitchell, ARL:UT
39	Susan G. Payne, ARL:UT
40	Clark S. Penrod, ARL:UT
41	Library, ARL:UT
42 - 78	Reserve, ARL:UT